AD-A147 909 BIO-OPTICAL VARIABILITY IN THE ALBORAN SEA AS ASSESSED BY NIMBUS-7 COASTA.. (U) NAVAL OCEAN RESEARCH AND DEVELOPMENT ACTIVITY NSTL STATION MS.. 1/1

UNCLASSIFIED P E LA VIOLETTE ET AL. AUG 84 NORDA-TN-283 F/G 8/1 NL

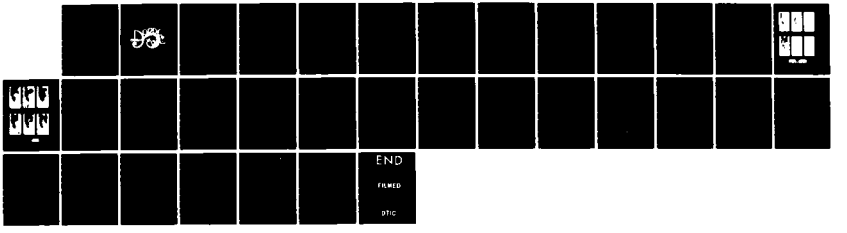

END

FILMED

DTIC

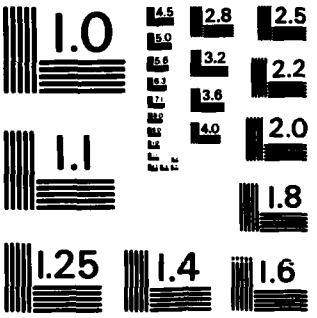

(12)

NORDA Technical Note 283

Naval Ocean Research and
Development Activity
NSTL, Mississippi 39529

Bio-Optical Variability in the Alboran Sea as Assessed by Nimbus-7 Coastal Zone Color Scanner

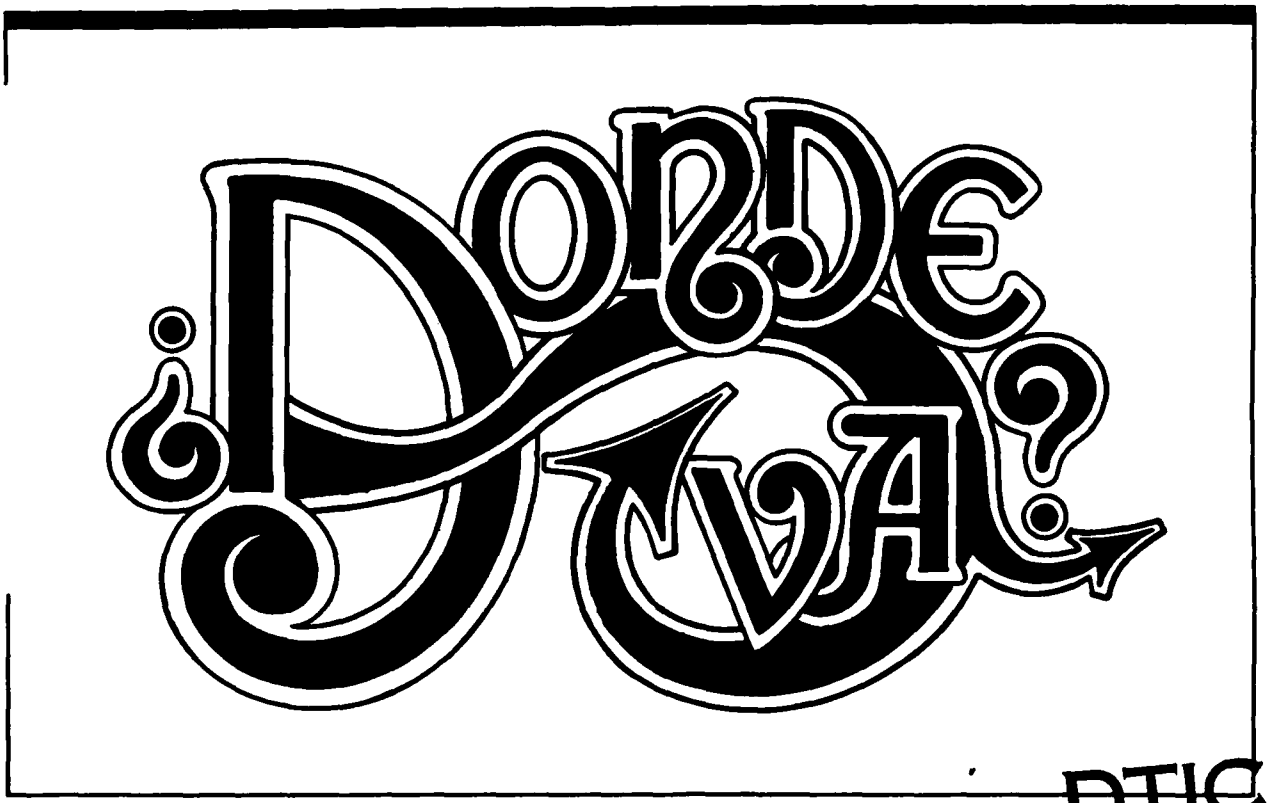

This paper has been submitted for formal publication
in the Journal of Geophysical Research.

Paul E. La Violette
Robert Arnone

Ocean Sensing and Prediction Division
Ocean Science Directorate

August 1984

ABSTRACT

An international oceanographic experiment, Donde Va?, was conducted in 1982 in the Alboran Sea in which a specialized portion was dedicated to examining the spatial and temporal variability of bio-optical properties around the Alboran Sea Gyre. The circulation of the Alboran Sea, as characterized by Atlantic Inflow (through the Strait of Gibraltar), the Alboran Gyre, and coastal water masses, was analyzed through use of Nimbus-7 Coastal Zone Color Scanner (CZCS) imagery, NOAA-7 Advanced Very High Resolution Radiometer (AVHRR) imagery, and aircraft and ship data. Diffuse attenuation coefficients calculated from CZCS data are in agreement with the ship data. A strong correlation between the surface temperature and ocean color fronts was observed in the two satellite imagery sets.

A 6-day sequence of CZCS imagery shows that significant changes in the diffuse attenuation coefficient and phytoplankton pigment concentration occurred in the frontal regions. These changes are attributed to the bio-optical horizontal and vertical variations that occurred within the first attenuation length.

ACKNOWLEDGMENTS

This research was supported by Naval Air Systems Command (PE 62759N WF 59553) and the Office of Naval Research (Code 422CS). Appreciation is extended to individual efforts and cooperation of the international members that composed the Donde Va? working group. The authors would especially like to thank Spanish scientists and crew aboard the B/S NAUCRATES. Special appreciation is also extended to Mr. S. Oriol III for technical assistance in digital processing. Personal thanks to Mr. R. Holyer, Drs. D. Wiesenburg and T. Kinder for review of the manuscript.

LIST OF ILLUSTRATIONS

BIO-OPTICAL VARIABILITY IN THE ALBORAN SEA AS ASSESSED BY NIMBUS-7 COASTAL ZONE COLOR SCANNER

I. INTRODUCTION

Donde Va?, an international oceanographic experiment conducted in the period June through October 1982 in the Alboran Sea, had as its major focus, understanding the regional circulation and the physical processes that force the dynamic changes (La Violette et al., 1982 and Kinder, 1983). Analysis of Nimbus-7 Coastal Zone Color Scanner (CZCS) data form a specialized portion of the experiment, which is aimed at determining the spatial and temporal variability of bio-optical properties associated with the circulation and the frontal dynamics. Preliminary results of this effort are described in this paper. An important aspect of the effort is an assessment of the utility of existing CZCS algorithms to obtain quantitative measurements of the optical diffuse attenuation coefficient and the phytoplankton concentration.

The West Alboran Basin is the first Mediterranean basin east of the Strait of Gibraltar (Figure 1). A 300-m sill located within the Strait forms the western boundary of the basin, and a series of subsurface ridges form the eastern boundary. Along the European and African coastal boundaries little shelf area exists, with the bathymetry dropping to depths of 1000 m approximately 5 km offshore.

The general circulation in the Alboran Sea has been characterized by several investigators (e.g., Lannoix, 1974; Parilla and Kinder, 1984; and La Violette, 1984). They describe the Atlantic water flowing into the Alboran Basin through the Strait of Gibraltar as essentially being confined to the upper 200 m. This water flows eastward along the Spanish coast for approximately 100 km, then turns southward toward a point slightly west of Cap Tres Forcas on the north African coast where it splits into a east-west flow. This circulation creates a large anticyclonic gyre (aptly called the Alboran Sea Gyre) that often occupies most of the West Alboran Basin.

The coastal water along the southern Spanish coast is cold, high in salinity, and rich in nutrients. Its complex nature is influenced by the movements of the Atlantic Inflow water as well as the local meteorology, bathymetry, and tides. La Violette (1984), using sea surface temperature values and patterns from thermal infrared satellite data, showed the Atlantic Inflow water has associated mesoscale cold-water thermal features that appear to be cyclic responses to the tides. La Violette and Kerling (1983), using aircraft expendable bathythermographs (XBTs), showed that the geographic location of the Atlantic Inflow is highly variable. The thermal characterization of the front formed between the waters of the cold Atlantic Inflow and the warm Alboran Sea Gyre is easily distinguishable by the gray shading of the thermal infrared satellite imagery. However, the demarcation between the northern edge of the Atlantic Inflow and the coastal water is difficult to determine since similar cold surface temperatures are present in both areas. The discrimination of the Coastal, Atlantic Inflow, and Alboran Sea Gyre waters should be improved by combining the analysis of color and thermal signatures of the water masses.

The large sea surface temperature variability such as described by La Violette and Kerling (1983) and La Violette (1984) indicates strong mixing or upwelling that should produce rapid changes in the amount of nutrients available for biological activity. In addition, the volume of the resulting biomass would depend largely on the time available for the organisms to respond to the advection or depletion of

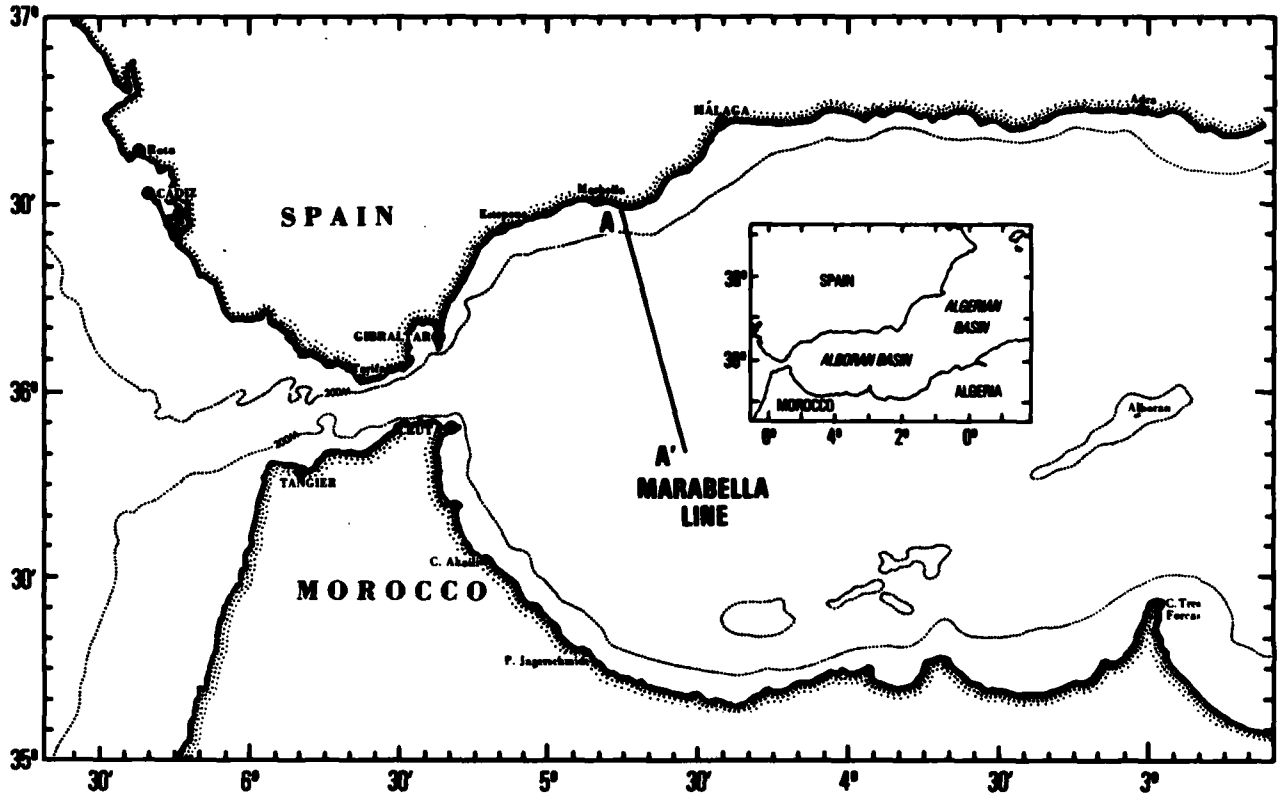

Figure 1: The Donde Va? study area in the Alboran Sea.

nutrients. Since water optical properties relate directly to the concentration of phytoplankton, their bloom (or decay) significantly changes the optical characteristics of the water. Thus, sequential CZCS iamgery should reveal changes in the surface bio-optical properties in a fashion similar to the temperature changes observable in sequential thermal IR imagery.

Before the data and their analyses are presented, certain basic premises must be emphasized. The upwelled radiance (or color) of the ocean results from backscatter within the water column combined with spectral absorption. Most important for these discussions, approximately 90 percent of the spectral water-leaving radiance at the surface is backscatter from within the first optical attenuation length (Gordon and McCluny, 1975). This length is defined to be the penetration depth at which the radiance falls to 1/e of its value just beneath the surface. For practical purposes, therefore, the upwelling spectral radiance at the water surface sensed by CZCS may be considered to be a result of the integrated effects of backscatter and absorption within the upper attenuation length, and that the amount of upwelled radiance from any depth deeper than the first attenuation length is negligible.

Figure 2 illustrates the inverse relationship of attenuation length with the diffuse attenuation coefficient, "k." Normally, for clear ocean waters, the attenuation length is 20 m or greater, whereas in coastal areas, the attenuation length is typically 2-4 m. Although the value of "k" depends on the vertical distribution of scattering and absorption properties, the value of the upwelling radiation does not reveal the depth at which the optical variability occurs. In other words, it is possible to have the same water-leaving radiance at the surface for two separate areas whose optical properties are vertically different within the first attenuation length (Gordon, et al. 1980b). A relatively turbid homogeneous water mass can display similar surface radiance as a clear water mass with a turbid layer within the attenuation depth. Thus, any vertical variation in the optic properties that occurs in the first attenuation length can have a significant influence on the upwelling water-leaving radiation sensed by the ocean color scanner.

The phytoplankton pigment concentration of ocean waters is largely responsible for the optical properties. This pigment is largely representative of chlorophyll a and also includes the phaeopigment concentration (Gordon, et al. 1983). The spectral absorption characteristics of the pigment has significant effects on the upwelling radiance at the sea surface and consequently on the signal sensed by CZCS. The strong correlation between this biological pigment and the water optical properties have been referred to as bio-optical properties.

II. COASTAL ZONE COLOR SCANNER IMAGERY

The Nimbus-7 CZCS is a 6-channel, multispectral scanning sensor having five narrow (+10 nm) visible channels centered at 443, 520, 550, 670, and 750 nm (Hovis, et al. 1978). The sensitivity of the spectral sensors is sufficient to measure subtle water color changes. The ground resolution at nadir is 800 m, and the satellite has a sunsynchronous noontime orbit so that for the Alboran Sea, three consecutive days of data collection are followed by 2 days when no data are collected. The satellite acquires data at approximately the same time each day, 11:30 hours local solar time.

The quantitative oceanographic analyses of CZCS data require that the data be calibrated in units of absolute radiance. Furthermore, a reliable method of separating atmospheric path radiance from ocean radiance is required. Gordon (1978) and

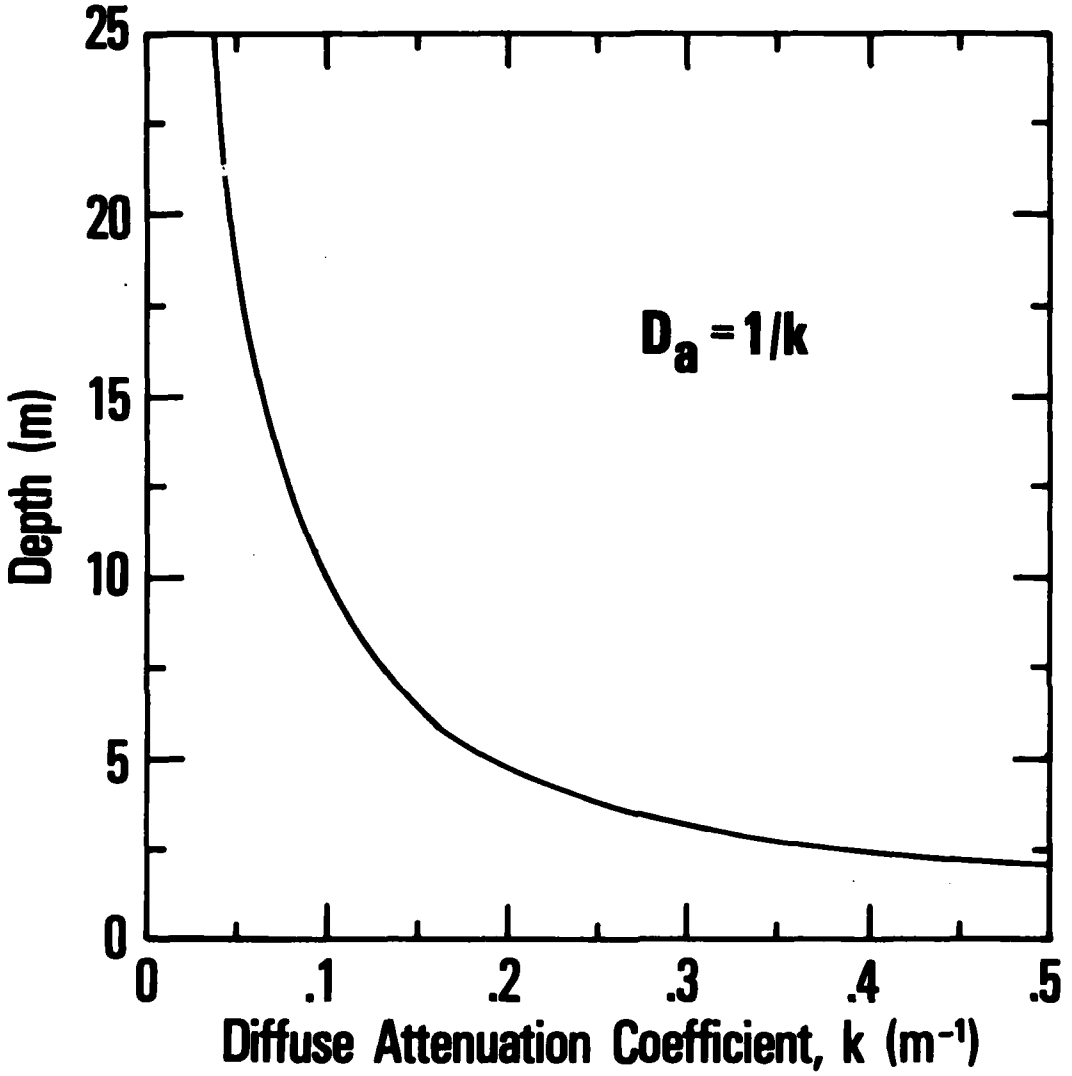

Figure 2: The inverse relationship between the diffuse attenuation coefficient (k) and the depth of the first attenuation length.

Gordon and Clark (1980a) developed a method that assumes the CZCS 670 nm channel can be used as a measure of the atmospheric aerosol concentration. Through a weighted subtraction of this channel with appropriate subtraction of Rayleigh scattering, the effective upwelling radiance from the ocean surface can be computed for the CZCS 443, 520, and 550 nm channels. However, there are several problems associated with this correction method that must be understood in relation to this study.

The first of these problems involves the proper selection of the Angstrom exponent. The Angstrom exponent relates the wavelength dependence of the aerosol optical thickness and single scattering albedo of the aerosols. (For a more complete explanation see Gordon and Clark, 1980a). Gordon and Clark (1981) suggests that in any CZCS image, the radiance values of clear water be used to obtain this value. However, this technique requires knowing the location of clear water areas within the CZCS image. Furthermore, the assumption is made that the Angstrom coefficient over the clear water is the same throughout the image. If this assumption is not valid, the selected Angstrom exponent value for one part of the image will produce erroneous values when applied to other portions of the image (Arnone, 1983). To overcome this difficulty, an improved method has been developed (Arnone and Holyer, 1984) in which selection of the Angstrom exponent is an interactive analyses procedure that defines the optimum coefficient for the entire image scene. This method was used for the sequential images presented in this study. It is interesting to note that the method showed that over the relatively small area of the Alboran Sea (300 by 200 km), the coefficient does not substantially change.

A second problem with this correction procedure is the assumption that water has zero upwelling radiance at 670 nm. This is a logical assumption for open ocean and shelf-type water masses where minimal concentration of suspended sediments occurs. However, significant upwelled radiance at 670 nm does occur in turbid coastal waters (Smith and Wilson, 1981; Arnone, 1983a; and Arnone, 1983b). For these coastal areas, an underestimation of the absolute upwelling radiance in the correct CZCS channels will result if this method is used. Fortunately, the waters of the Alboran Sea are relatively clear and only in data from very nearshore waters (1-3 km) should errors arise.

The final (and potentially most significant) problem with extracting quantitative results from CZCS data comes from uncertainties in the radiance calibration coefficients of each of the spectral channels. The sensor sensitivity of the CZCS has been decaying since launch with the result that the original calibration coefficients are no longer applicable (Austin, 1982; Sun, 1983; and Gordon, et al., 1983). For the Alboran Sea analyses presented here, an exponential decay of the sensitivity of the CZCS spectral channels has been implemented that extends from the time of launch to the time of the Alboran Sea data set (Goddard Space Flight Center, Systems and Applied Science Corporation, personal communication). In addition, for the short period of the CZCS imagery presented here, the decay rate is insignificant when comparing individual images.

In this study, the ratio of the absolute upwelling radiance for the 443- and 550-nm channels (i.e., 443/550) is used to derive both the diffuse attenuation coefficient "k" at 490 nm (Austin and Petzold, 1980), and the phytoplankton concentration (Gordon and Clark, 1980a). This method implies an inherent relationship between "k" and phytoplankton concentration. While this relationship would be expected in the open ocean and shelf waters, there are limitations in coastal areas where "k" may be heavily influenced by suspended sediments (Arnone, 1983a; and Arnone, 1983b). As mentioned earlier, the Alboran Sea is comparatively clear

although problems with high sediment concentrations could occur only within 1 to 3 km of the coasts.

The CZCS imagery presented throughout this study is displayed as the absolute value of the ratio of the 443- to 550-nm channels. In addition, the imagery has been geometrically registered to a Mercator projection with a registration accuracy of ± 1 km. Thus, reliable measurements may be made of the temporal variability between sequential images. As an aid to both clarity and location, a land mask of the area with the appropriate latitude/longitude grid is superimposed on the imagery. The image processing was done on an interative digital satellite processing system located at the Naval Ocean Research and Development Activity.

III. SURFACE DATA COLLECTION

Shipboard measurements of optical and biological parameters were collected along a line extending south from Marbella, Spain, (lat. 36°28'N, long. 4°47'W) to the approximate center of the Alboran Gyre (lat. 35°52'N, long. 4°35'W) (Figure 1). This line, called the Marbella Line, was designed to transect the Coastal, Atlantic Inflow, and Alboran Sea Gyre waters.

The dates of the various in situ parameters along the transect during the experiment are tabulated in Table 1.

TABLE 1. Data Summary During Experiment

	October 1982										
Parameters	4	5	6	7	8	9	10	11	12	13	14
Beam transmittance				X				X	X		X
Conductivity/temperature				X				X	X		X
Spectral diffuse attenuation coefficient				X				X	X		
XBT	X	X			X	X		X		X	X
Chlorophyll-A				X	X	X		X	X	X	X
Suspended sediments				X	X	X		X	X	X	X
PRT-5-radiation temperature	X	X		X	X	X		X	X	X	X
CZCS coverage			X	X	X			X	X	X	

Beam transmittance was measured with a modified Martek Instrument integrated with a desk top calculator. The spectral response of the instrument was centered at 490 nm (+10 nm). The instrument is considered reliable to 1 percent transmission. The instrument was lowered to a depth of 50 m while continuously measuring percent-transmission and temperature.

The spectral diffuse attenuation coefficient was measured by an optical instrument specially designed by Research Support Instruments. The instrument consisted of a deck unit and a submersible unit both equipped with a photon counter and a monochromometer for scanning the visible spectrum between 400-800 nm. The submersible unit was equipped with an upward and downward looking window, both viewed through cosine collectors to measure upwelling and downwelling irradiance. The unit was

controlled by a HP-85 calculator and operated in a scanning and time averaging mode. Upward and downward spectral "k" measurements were integrated over the depth of one attenuation length.

Chlorophyll and suspended sediment concentration measurements were made along the Marbella Line at discrete bio-optical stations. Techniques of instrumentation and analyses were outlined in Garcia, et al. (1983). Chlorophyll analyses included both continuous flow through fluorometric techniques (in-vivo) and extraction techniques from in situ water samples at discrete depths. Suspended sediment analyses were done by filtration and grammetric procedures on water samples collected from depth and continuous surface samples.

The subsurface thermal structure derived from data analyses obtained from XBTs and thermal sensors on the optical instrumentation provided the basis for locating the bio-optical stations within water masses and to couple the surface measurements with the subsurface oceanography.

IV. RESULTS AND DISCUSSIONS

A. Coastal Zone Color Scanner Imagery

Atmospherically-corrected CZCS imagery registered to a Mercator projection for six sequential days (6, 7, 8, 11, 12, 13 October 1982) are presented in Figure 3. The imagery represents the ratio of the 443- to 550-nm channels with the color table applied in the figure. From ratio values, the diffuse attenuation coefficients, and phytoplankton pigment concentrations (referred to as Chl on the figure), are illustrated in this figure. (Note that the color scales are not a linear relationship of "k" and pigment concentrations.) The color scale represents higher turbidity coastal water masses as brown, shelf- type waters as yellow to green, and clear oceanic waters as blue.

In the CZCS imagery, the Alboran Sea Gyre is observed to have low "k" values and low phytoplankton concentration (blue). The gyre is encircled by waters of elevated turbidity and phytoplankton concentration especially along its northern and eastern frontal boundaries. The result is a ribbon of significant color gradient that is observed to move eastward in the 6 to 8 October imagery. (The changing color intensity of the front will be discussed in the following section.) On 11 October, the frontal characteristics appear significantly different, especially on the eastern boundary where the ribbon appears to have become more diffuse. The 12 and 13 October images show complex sinuous features developing within the frontal region. The 13 October image also shows the farthest eastward frontal position, located slightly to the west of Cap Tres Forcas.

The general water mass features seen in the CZCS imagery are also observable in the same locations in the NOAA-7 infrared imagery for the same period (Figure 4). Analyses of the infrared imagery during the ?Donde Va? experiment by La Violette (1984), indicate that a series of submesoscale cold water tongues were advected clockwise around the gyre. This phenomenon is also observable in the CZCS imagery in Figure 3. Originating at the Strait of Gibraltar, turbid water masses are shown to enter coincident with cold water tongues that develop as part of the Atlantic Inflow. In the infrared imagery for the following days, the tongue is advected around the periphery of the gyre. In the 12 October image, the start of one of the features is readily observed as the yellow coloration apparent within the strait. Upon entering the Alboran Sea, these turbid water tongues of Atlantic Inflow water

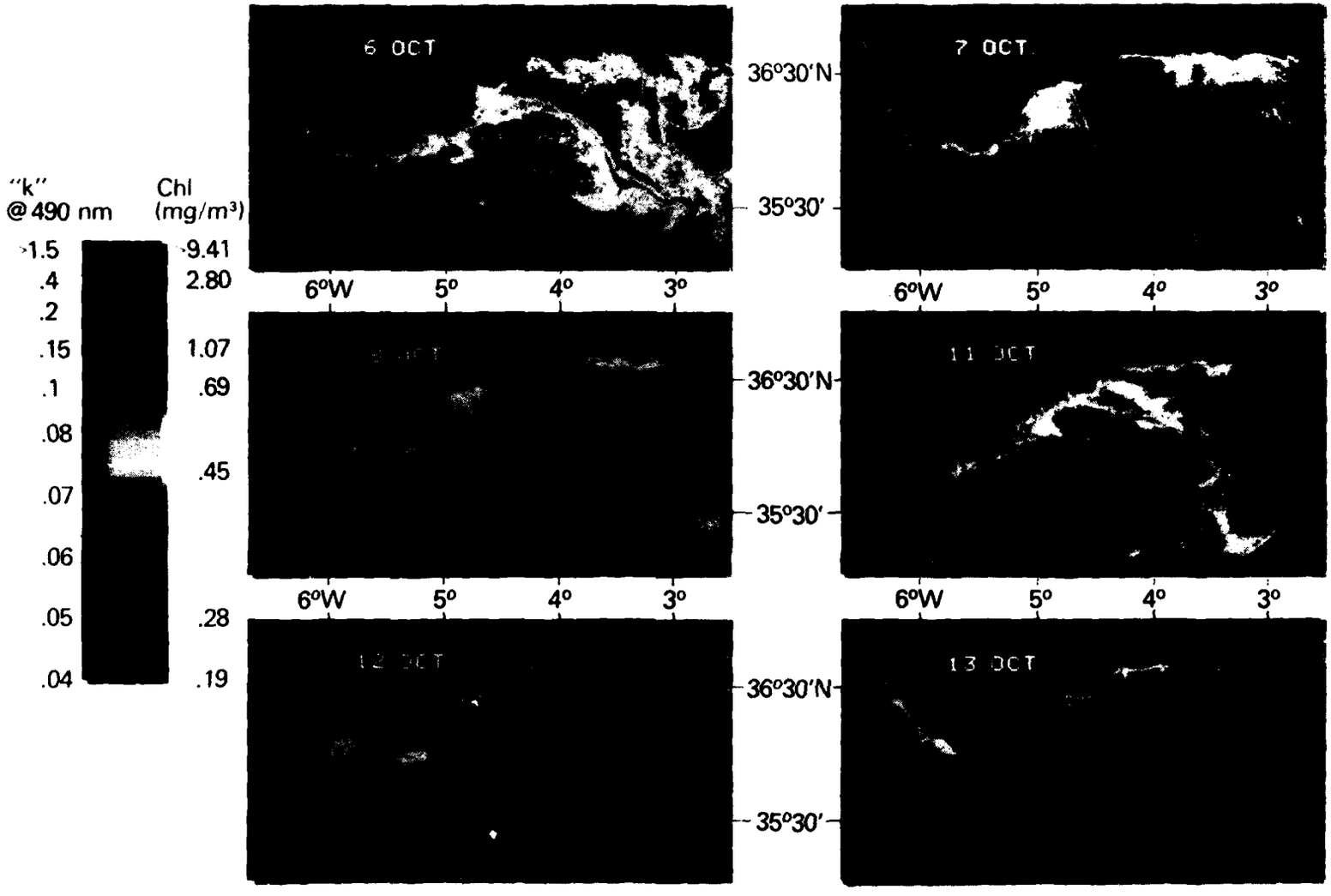

Figure 3: Atmospherically-corrected and spectrally ratioed (443:550 nm) sequence of Nimbus-7 CZCS imagery showing quantitative biooptical properties.

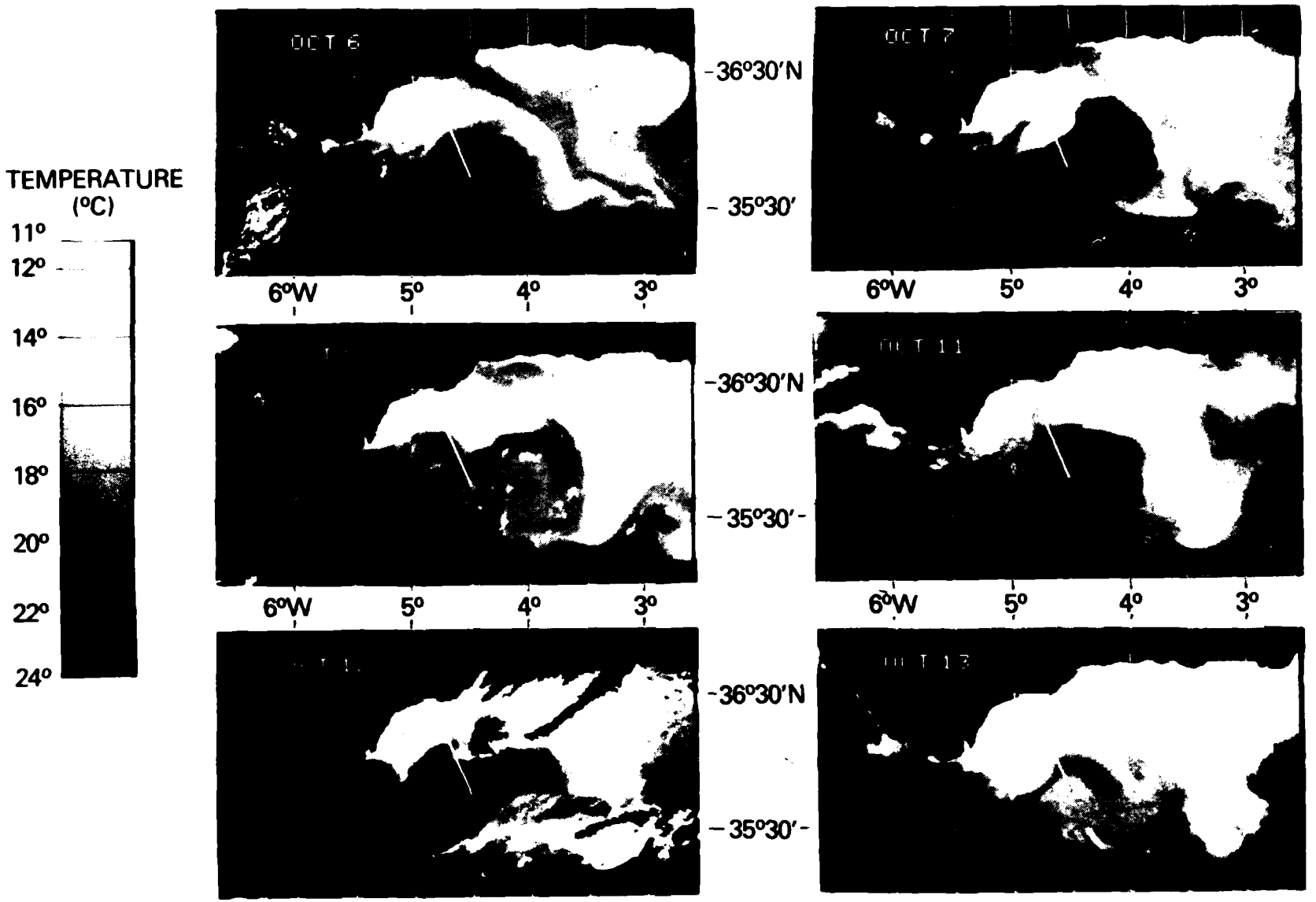

Figure 4: Atmospherically-corrected sea surface temperatures from NOAA-7 AVHRR imagery coinciding with the CZCS imagery shown in Figure 3.

are not readily distinguishable in color from the color of the coastal water, which also appears turbid with elevated phytoplankton concentrations. As each particular feature continues its eastward migration, it maintains its identity and sharp frontal boundaries. Note that several of these turbid, submesoscale tongues can be observed in a single image. Their initial speed appears to be slow near Gibraltar and to increase to an average speed of approximately 40 cm/sec as they move around the gyre. The cyclic appearance of these tongues appears to be about 12 hours and is believed to be related to tidal movement through the Strait of Gibraltar (La Violette, 1984).

The coastal waters bio-optical properties surrounding Cap Tres Forcas rapidly change in the Figure 3 imagery. The 7 and 8 October imagery show small westward flow of the coastal waters as a turbid plume. On 11 October, however, the plume developed into a thin ribbon of higher turbidity water propagating northwestward approximately 100 km offshore.

It is interesting to note that in the Atlantic, the coastal waters along the western Spanish coast are characterized by high turbidity and phytoplankton concentration in all six images. The Rio Guadalquivir is shown to discharge high suspended sediments and nutrients into the Sea of Cadiz. In the sequence of imagery, this turbid water mass appears to enter the Alboran along the northern side of the Strait of Gibraltar and may be a major source of nutrients for the biological processes taking place within the Atlantic Inflow water.

The most striking feature of the CZCS sequence is the extreme color changes that occur from 1 day's image to the next. Note that color gradients define the frontal positions of the water masses in all of the imagery. However, the actual color values in each image show strong changes that must represent changes in upwelling radiation (assuming no errors introduced by atmospheric correction). This, in turn, implies that optical or biological changes have occurred within the first attenuation length. The reddish ribbon of Atlantic Inflow water in the 6 October image changes to a light blue ribbon in the 7 October image, and is barely visible in the 8 October image. This indicates a day-to-day change of the diffuse attenuation coefficient from 0.15 to 0.07 to 0.06 or a phytoplankton decrease of from 1.05 to 0.45 to 0.35 mg/m^3. A similar progression, though not as dramatic, may be observed to occur in the 11 to 12 October imagery, where "k" values decreased from 0.09 to 0.075 (little change is found in the 13 October image.). Notice that the Atlantic coast shows high turbidity in all of the images.

A reevaluation of the atmospheric correction process indicates that an inherent error might be responsible for the large temporal variability. The Angstrom exponent selected for each spectral channel in each image could create variability in the absolute upwelling radiance values. If this were true, then a relationship must exist between the Angstrom exponent and the upwelling radiance. To test the validity of this relationship, a pixel located approximately 6 km off of Marbella, Spain, was selected. The absolute upwelling radiance for the three channels (443, 520, and 550 nm) and the associated Angstrom exponent used for the atmospheric correction process for each of the six CZCS images was plotted (Figure 5). The obvious lack of correlation in the plotted data indicates the observed color changes are not the result of the selection of the Angstrom exponent. Thus, the Angstrom exponent selection in atmospheric correction process is not the cause of the color variability apparent in the imagery.

Notice that in Figure 5 the upwelling radiance normally associated with suspended sediment concentration (550 nm) is clustered around 0.038 W/cm^2 +.004. The compact nature of this cluster suggests that the suspended sediment concentration had minimal changes at this location in all six images. Conversely, the large changes in the upwelling radiance in the 443-nm channel (0.074-0.032 W/cm^2) indicate that upwelling radiance values in this spectral image were primarily responsible for the color variability. Since the 443-nm channel is normally associated with chlorophyll absorption, the daily changes observed appear to result from actual chlorophyll variability.

The large daily changes in the absolute upwelling spectral radiance could be a result of several factors. They could be a result of either the rapid bloom (or decay) of large phytoplankton concentrations in the upper layers of the ocean, or the upward migration or upwelling advection (or sinking) of the phytoplankton populations. The growth rate of phytoplankton is dependent upon nutrient availability, temperature, zooplankton grazing, and irradiance distribution. Cullen and Eppley (1981) found that the phytoplankton concentrations can double per day for a specific vertical depth. As a result, phytoplankton concentrations can change both horizontally and vertically with time. However, only those changes that occur within the first attenuation length affect the spectral upwelling radiance sensed by visible remote sensors.

B. Ship Data along the Marbella Line

Cross sections along the Marbella Line of temperature, beam transmittance, chlorophyll, and suspended sediment concentration are presented in Figures 6 and 7 for 11 and 12 October. The temperature section on 11 October (Figure 6) shows that a sharp surface front that sloped to the south was present 15 km from the coast. The beam transmittance cross section for 11 October closely resembles the temperature cross section. The surface transmittance front corresponds to the thermal front, increasing from 70% at the coast to 80% at the front. Further offshore, the water became even clearer, with transmittance values of 90+%. The vertical distribution of transmittance values shows an upward intrusion of clear 90+% water occurred at 25-m depth 25 km from shore. This clear water approached the coast at approximately 50 m, underlying the more turbid coastal waters. Again the isotherms also showed a similar trend indicating strong interrelationship.

The 11 October chlorophyll cross section in Figure 6 shows distributions similar to that of beam transmittance and temperature. Surface chlorophyll concentrations change at the surface front from 0.3 to 0.2 mg/l., with higher chlorophyll values observable at depth. The strong chlorophyll front corresponds to the 90% isoline of beam transmittance in the area of the upward intrusion of the clearer waters. In the coastal waters, the upper 35 m contain high chlorophyll concentrations, while at depth the exceptionally clear water are shown associated with extremely low temperature water.

The 12 October temperature cross sections in Figure 7 show significant variations from the previous day. The surface thermal front has dissipated and a gradual temperature change from 17 to 19^{o}C is observed out to 50 km offshore. The warm (>20^{o}C) surface waters of the gyre are not seen in this section, although a gentle southern dipping of the isotherms are observed. The change in beam transmittance for the 12 October cross section is similar to that of temperature. Low transmittance (80%) measurements are observable 40 km from the coast. The isolines of beam transmittance like those of temperature slope down to the south.

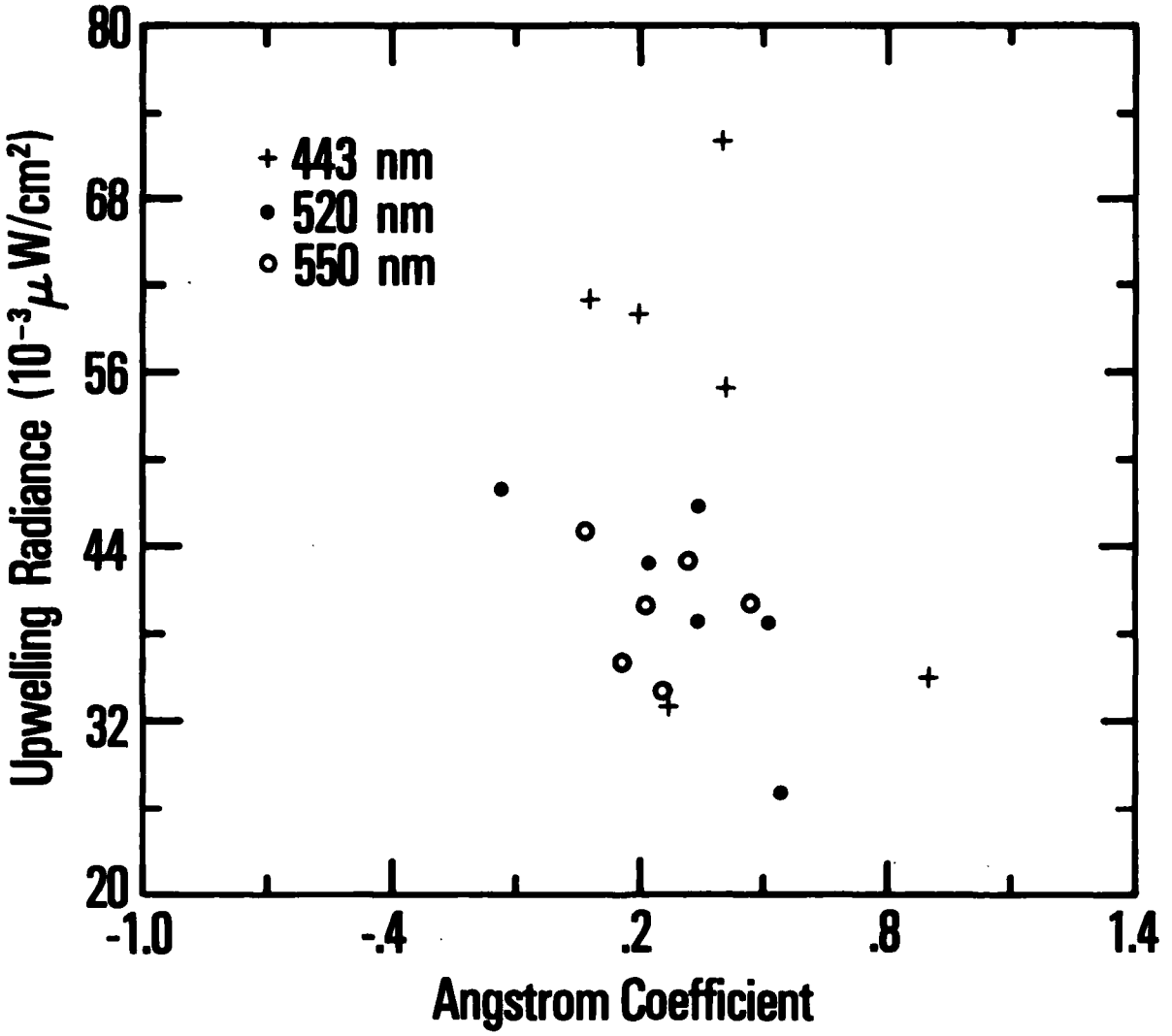

Figure 5: Water-leaving radiance calculated from CZCS at a single pixel location and the Angstrom coefficient used in atmospheric correction for the spectral channels.

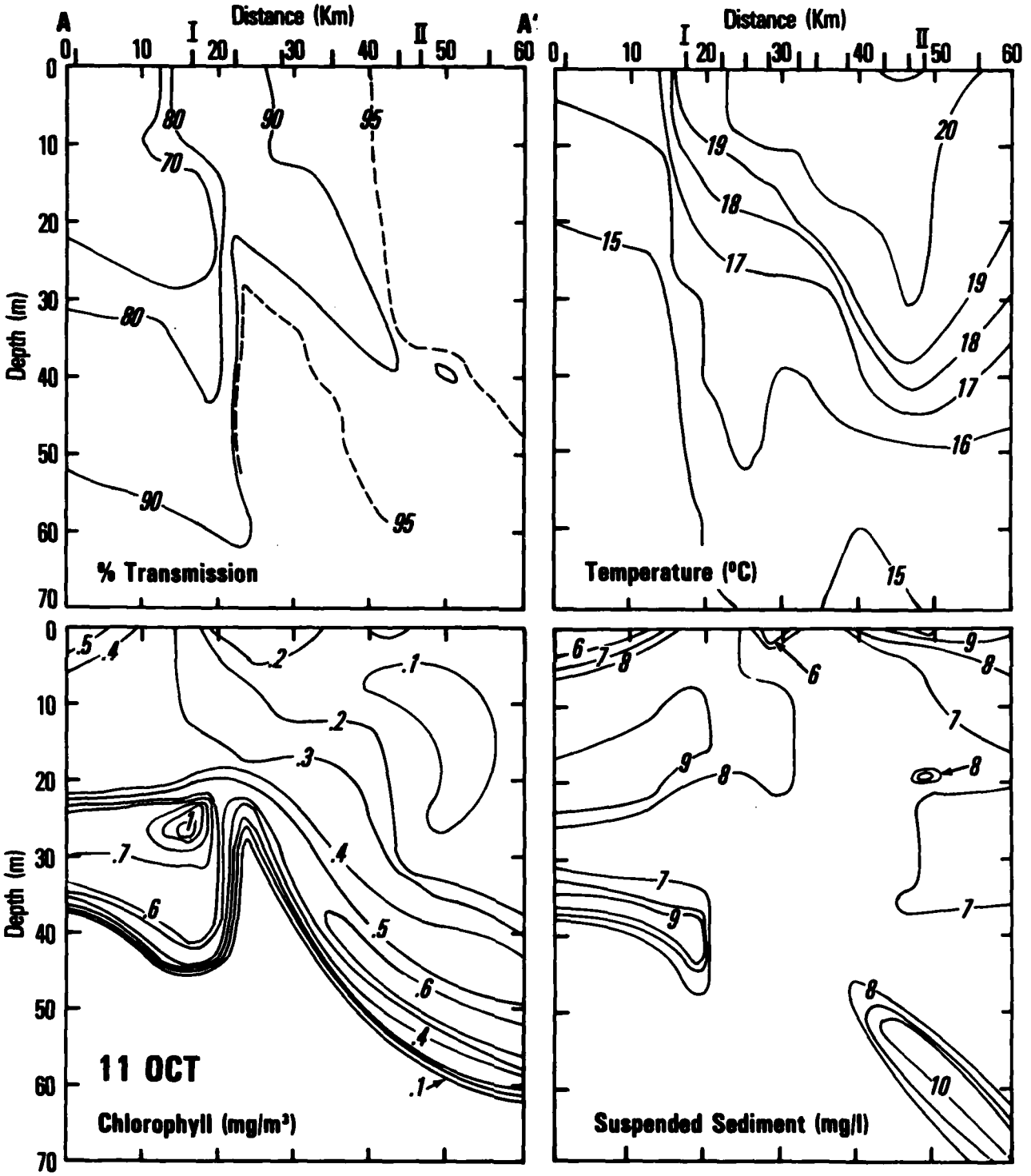

Figure 6: Cross sections along the Marbella Line on 11 October.

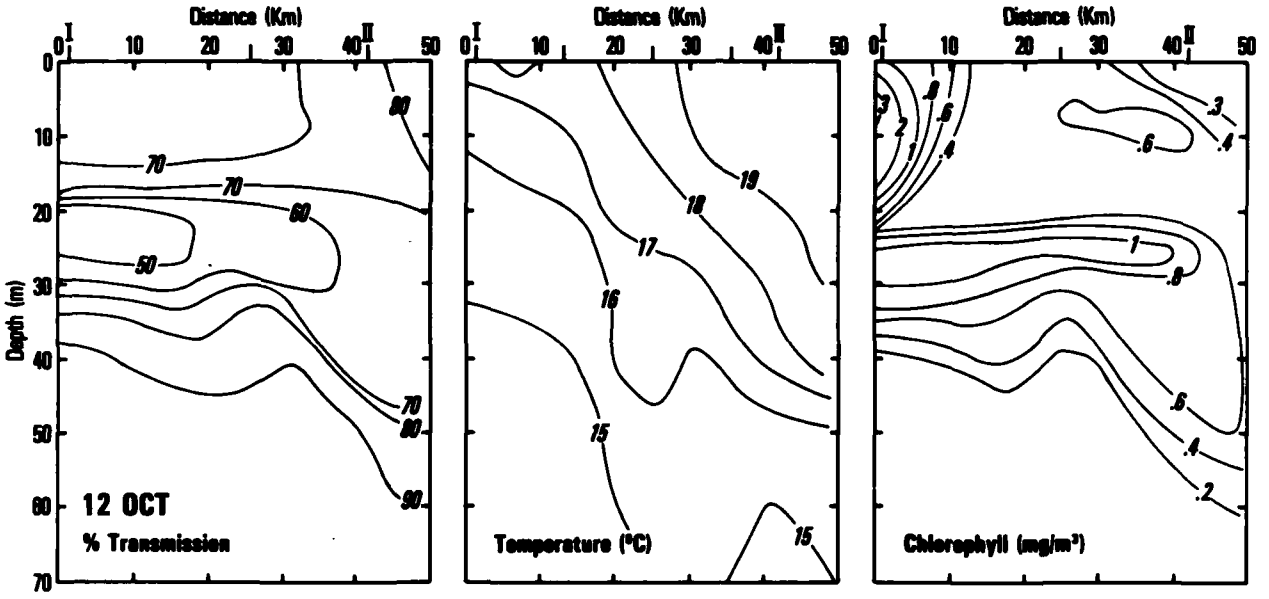

Figure 7: Cross sections along the Marbella Line on 12 October.

The cross section of the chlorophyll concentration for 12 October also shows a significant change from the previous day. The section shows exceedingly high values in excess of 2 mg/m^3 close to the coast in contrast to the 0.5 mg/m^3 the previous day. Surface waters 40 km from the coast have concentrations of 0.3 mg/m^3 compared to 0.1 mg/m^3 the previous day. At 25-m depth, a major vertical chlorophyll concentration change occurs. Maximum values of 1 mg/m^3 are illustrated to extend offshore to 40 km on 12 October. The previous day this value of 1 mg/m^3 extends only 18 km offshore. Notice that at 35 m low chlorophyll values are observed on 11 and 12 October indicating that temporal variability appears confined to the surface waters.

The changes in beam transmittance, temperature, and chlorophyll concentration for these 2 days indicate that an apparent southern movement of the upper 30 m of water takes place in 24 hr. The cause of this movement, as well as the direction of actual displacement, will be discused in the following section when the vertical sections of the ship data are related to the horizontal displays of the satellite data.

It is important to note that the vertical profiles of beam transmittance provide a clue to the relationship of optical property variations in the first attenuation length and the visible, remote sensing signals.

Vertical profiles of beam transmittance along the Marbella Line are illustrated in Figures 8 and 9 for 11 and 12 October. The four profiles in Figure 8 are representative of different water masses beginning near the coast (1) and ending offshore in Alboran Gyre water (4). The Alboran Sea Gyre water has high transparency (97%) and is relatively homogeneous to its first attenuation length of 21 m. Profile (3) representing the southern side of the Atlantic Inflow water, has reduced transmissivity (90%) and a nonhomogeneous upper layer. Decreasing transmissivity is observed from the surface with a slightly turbid layer (88%) existing at 12 m. The first attenuation length extended into the upper 2 m of this layer such that the water-leaving radiation has a spectral component that arose from within this layer.

Profile (2), located north of the Atlantic Inflow, has reduced transmissivity (83%) and shows a significant variation within the first attenuation length. The upper 10 m is optically homogeneous. A sharp decrease in transmissivity from 85 to 70% occurs between 10-12 m. The 70% transmissivity layer extends to 29 m where an abrupt increase to 92% transmissivity occurs with depth. The first attenuation length extends to 17 m and is partially inclusive of the 70% transmissivity layer.

The final profile (1) located just offshore of Marbella at the start of the Marbella Line has reduced transmissivity in the upper 5 m (67%). The increase and rapid decrease in transmissivity with depth indicates a complex optical nature within the upper 35 m. However, since the first attenuation length is confined to the upper 8 m, most of this complex vertical structure does not substantially influence the water-leaving radiation and, hence, is not represented in the CZCS data.

Figure 9 representing profiles for 12 October illustrates a profile located within the same coastal water mass (profile 1) as the previous day. Within the first attenuation length of 8-m, surface transmittance (65%) decreases to 60%. The strong vertical variations have a similar shape to the previous day. However, these are also outside the depth detectable by the CZCS sensors. In comparing the 11 and 12 October profiles, note that the vertical variations of the optical properties have a direct influence on the depth to which the CZCS sensor can receive its signal.

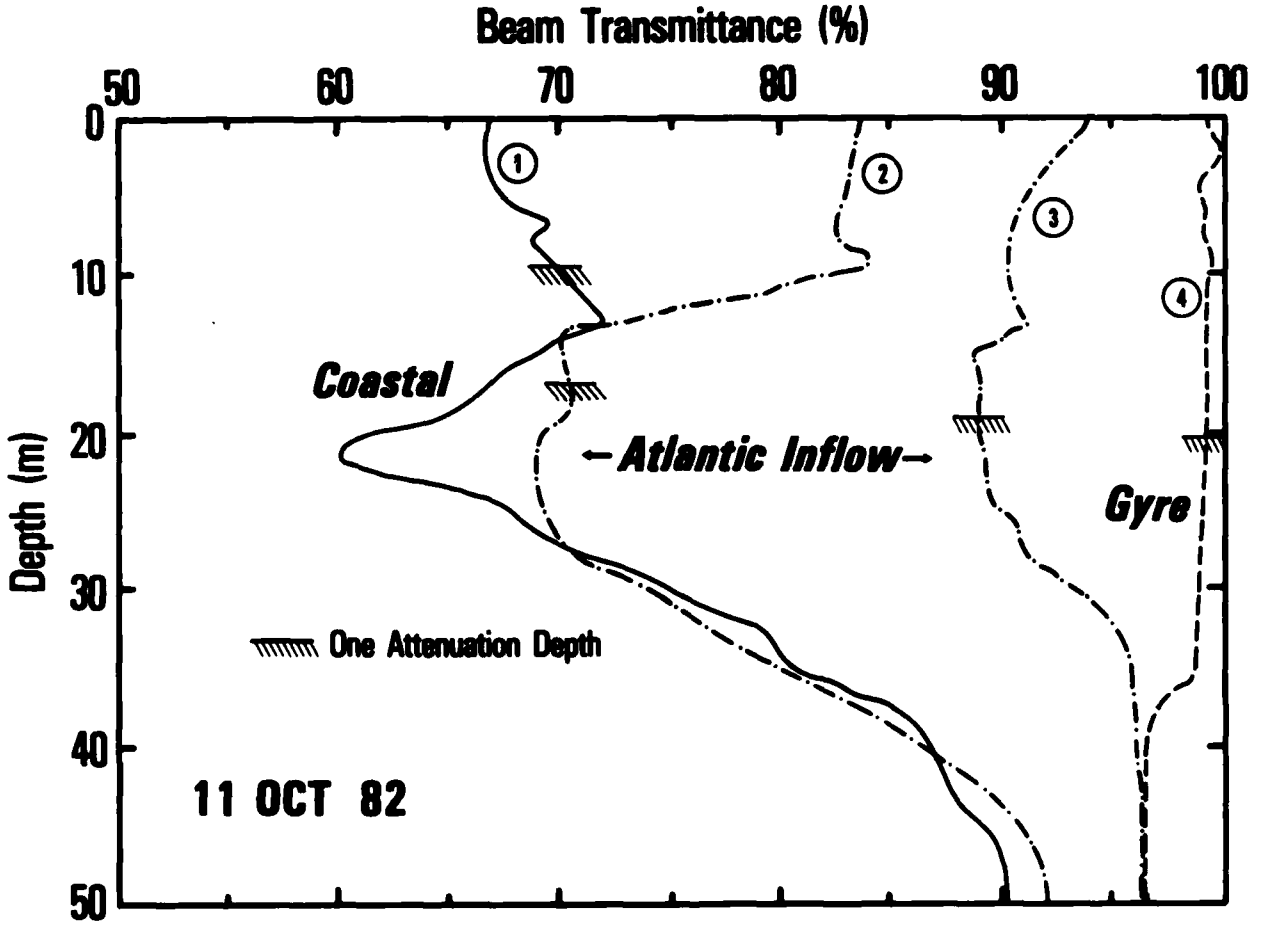

Figure 8: Vertical profiles along the Marbella Line of beam transmittance on 11 October.

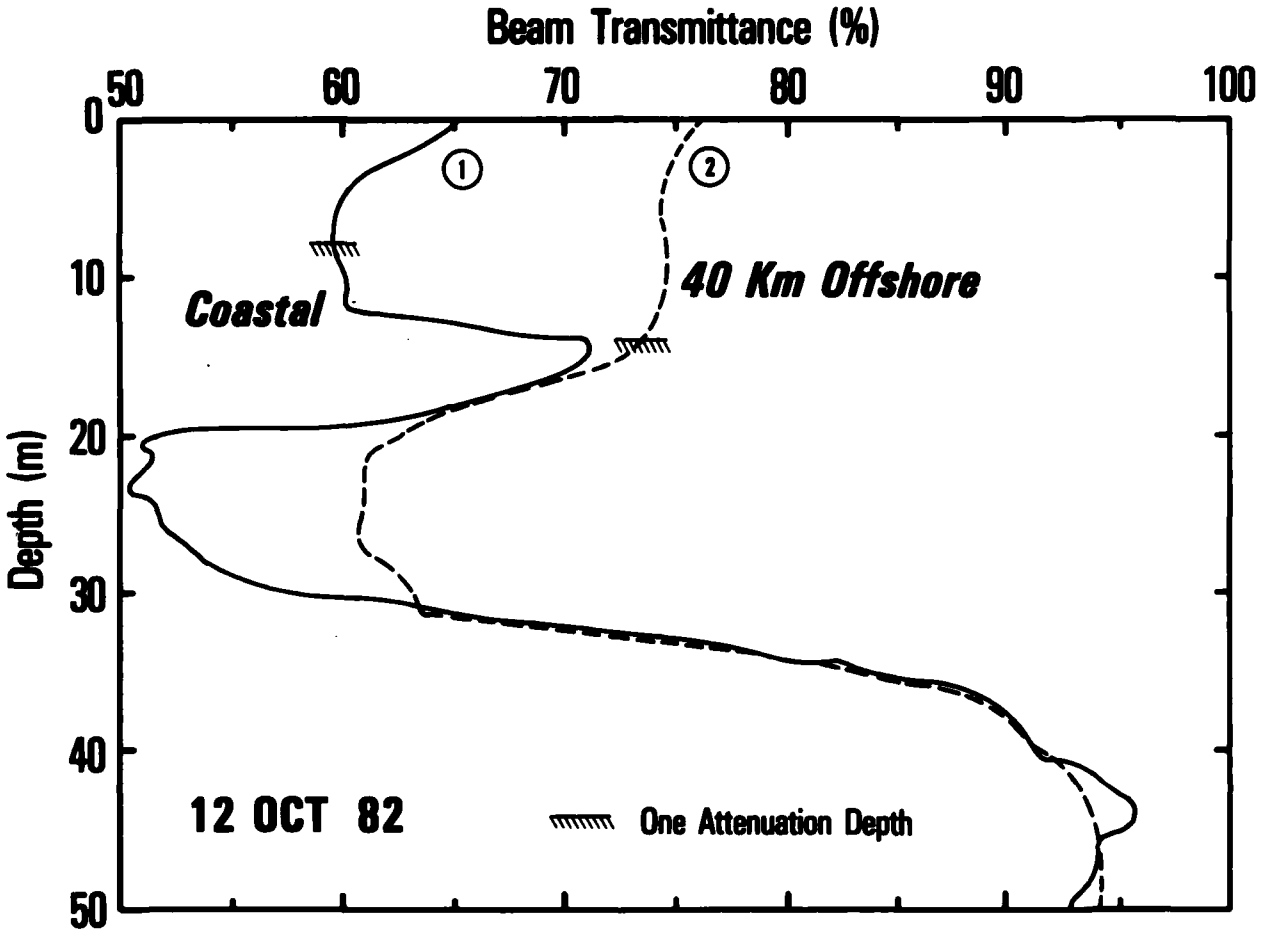

Figure 9: Vertical profiles along the Marbella Line of beam transmittance on 12 October.

Profile (2) in Figure 9 is observed 40 km offshore in a similar location as profile (3) for 11 October (Figure 8). Profile (2) exhibits an optically homogeneous water mass to 14 m, which is also the first attenuation length. A lower transmissivity layer (60%) is observed between 18 to 32 m. Through comparison with the previous day, the shape of profile (2) is similar to waters found closer to shore.

From this it can be seen that the vertical variations of the optical properties have significant influence on the upwelling radiation detectable by the CZCS visible range spectral sensors. Since the signal is basically confined to the first attenuation length of the water column, the movement of the vertical optical layers into and out of this attenuation length will result in different measurements of upwelled radiance. The difficulty is further compounded since these movements may change the depth of the first attenuation length. All of this contributes to the high temporal variability observed in the sequence of CZCS imagery in Figure 3. An important fact to be reemphasized is that changes below the first attenuation length will not be detected by the visible range sensors.

C. Comparison of Satellite and Ship Data

The movement of the coastal water noted in the ship data is also observable in the 11 and 12 October satellite data. The two data sets show that the complex vertical bio-optical properties in the upper water mass are likely to have been responsible for the high temporal and spatial variability observed in the sequential CZCS imagery. Most important, the two data sets add critical dimensional information to one another. For example, the cross sections provided by the ship data along the Marbella Line are much more informative when placed in position in the horizontal frame of the satellite data. Now, the apparent rapid southerly movement of the coastal water mass previously observed in the ship data can be seen to be actually attributable to an eastward advection of the highly turbid, cold water feature observable crossing the Marbella Line in the 11 and 12 October satellite imagery. The ship data, in turn, adds vertical dimension to the satellite display by showing that the distribution of bio-optical properties is in the upper 30 m.

The spectral upwelling and downwelling diffuse attenuation coefficients for 11 and 12 October are illustrated in Figures 10 and 11. These spectral measurements represent the water mass variations across the Marbella Line coastal (I) and 40 km offshore (II) on 12 October, Inflowing Atlantic water (I), and Alboran Gyre (II) on 11 October. (The positions of these stations are shown in Figures 6 and 7.) A shift in wavelength for maximum light transmission occurs in progressing north from the waters of the gyre to the Spanish coast (490 to 550 nm) in addition to an increase in the diffuse attenuation coefficient values.

The diffuse attenuation coefficient at 490 nm (computed from the CZCS data) are compared to ship observations in Figure 12. There are difficulties in this comparison. First, the optical properties of the regional water masses exhibited high spatial variability within the 800-m resolution of the CZCS imagery. This is further compounded by the 1-2 km registration accuracy of the satellite processing (the ship naviagation also contained +2 km position errors when more than 10 km offshore). In addition, many environmental affects such as sea state conditions, solar altitude, and ship shadow can contribute as much as 10% error to the ship data. Despite all of these factors the ship and satellite data show good agreement.

A similar comparison of the phytoplankton concentration calculated from CZCS and ship measured values of the surface waters illustrated in Figure 13 also shows

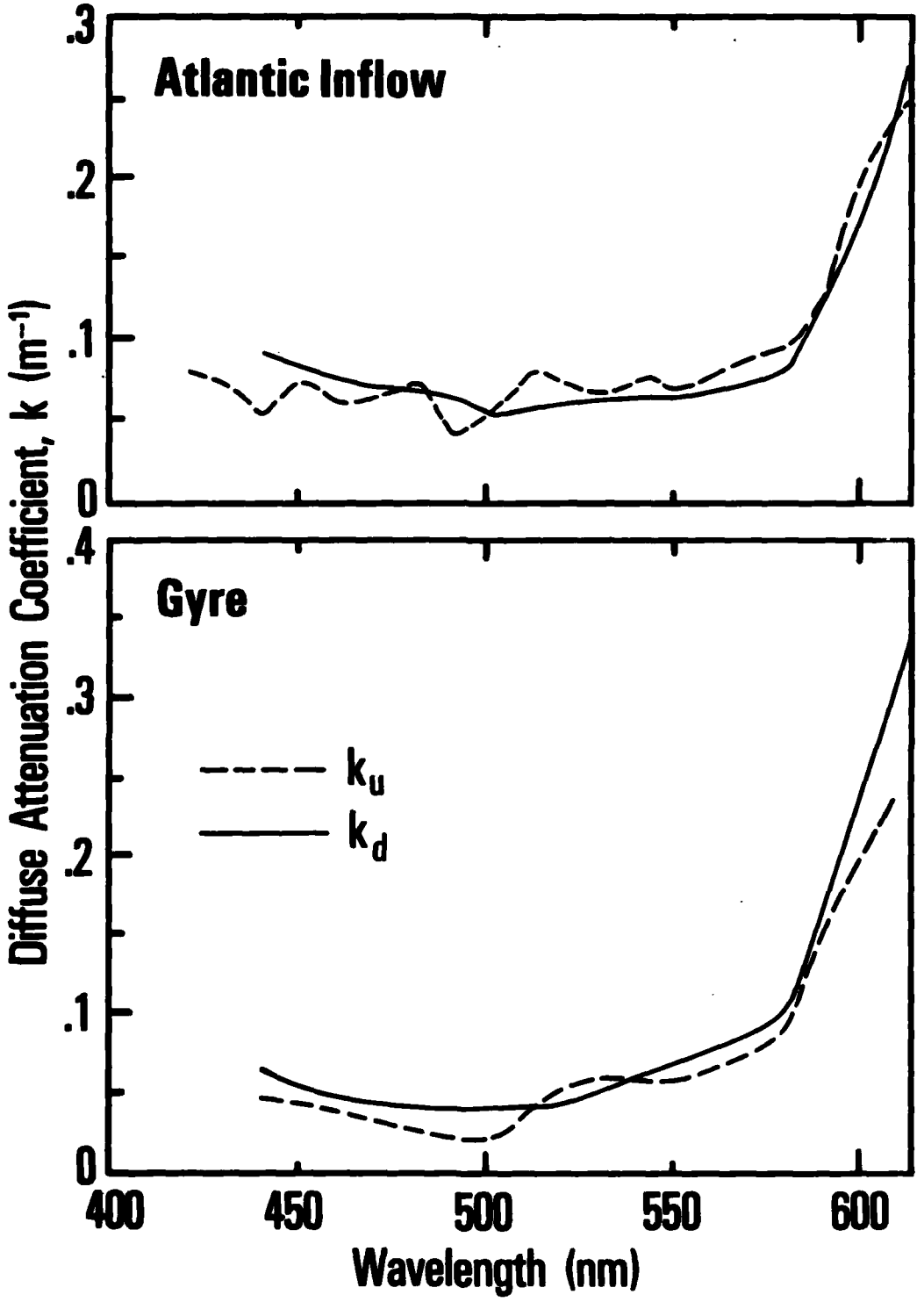

Figure 10: Spectral diffuse attenuation coefficients along the Marbella Line on 11 October.

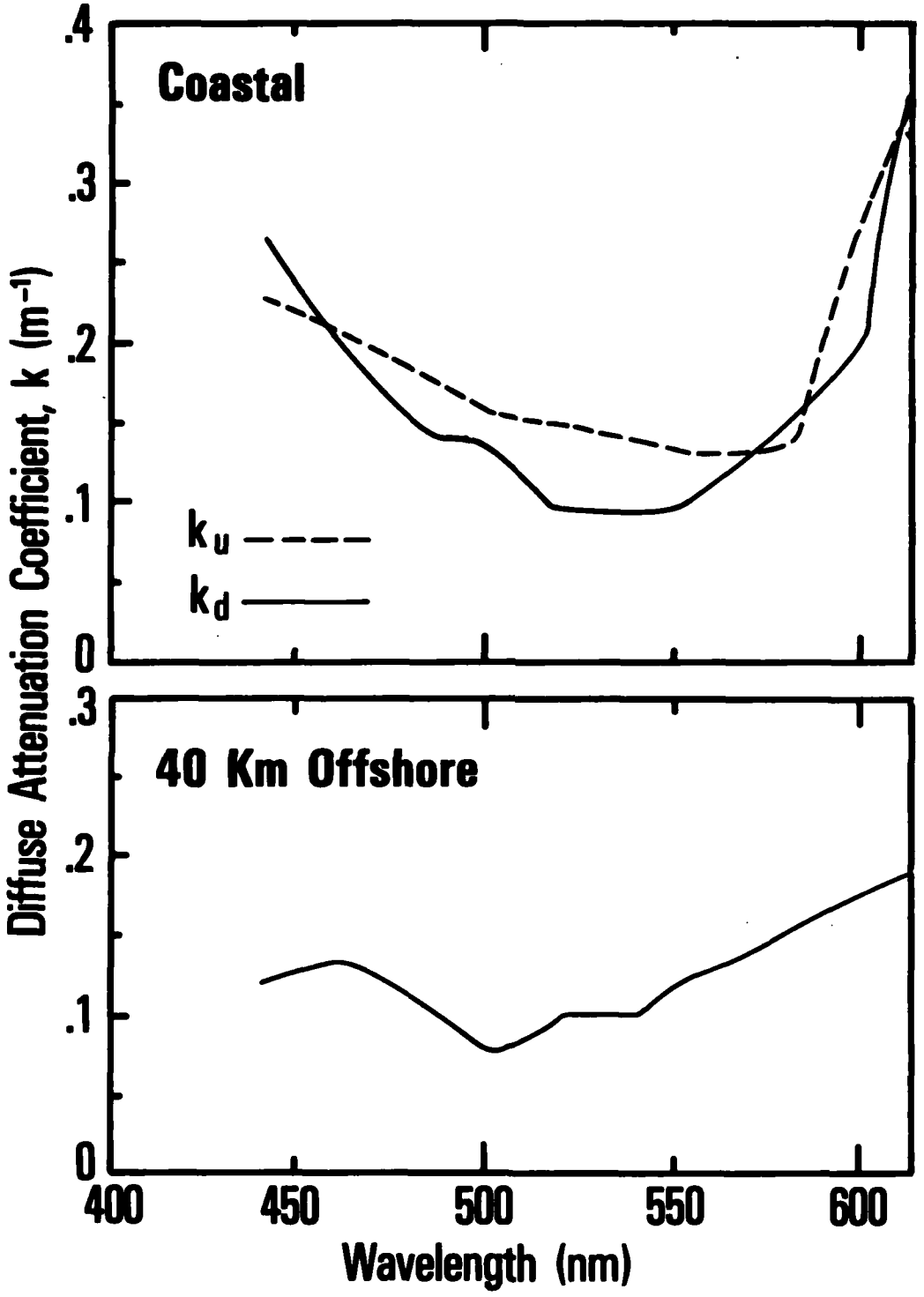

Figure 11: Spectral diffuse attenuation coefficients along the Marbella Line on 12 October.

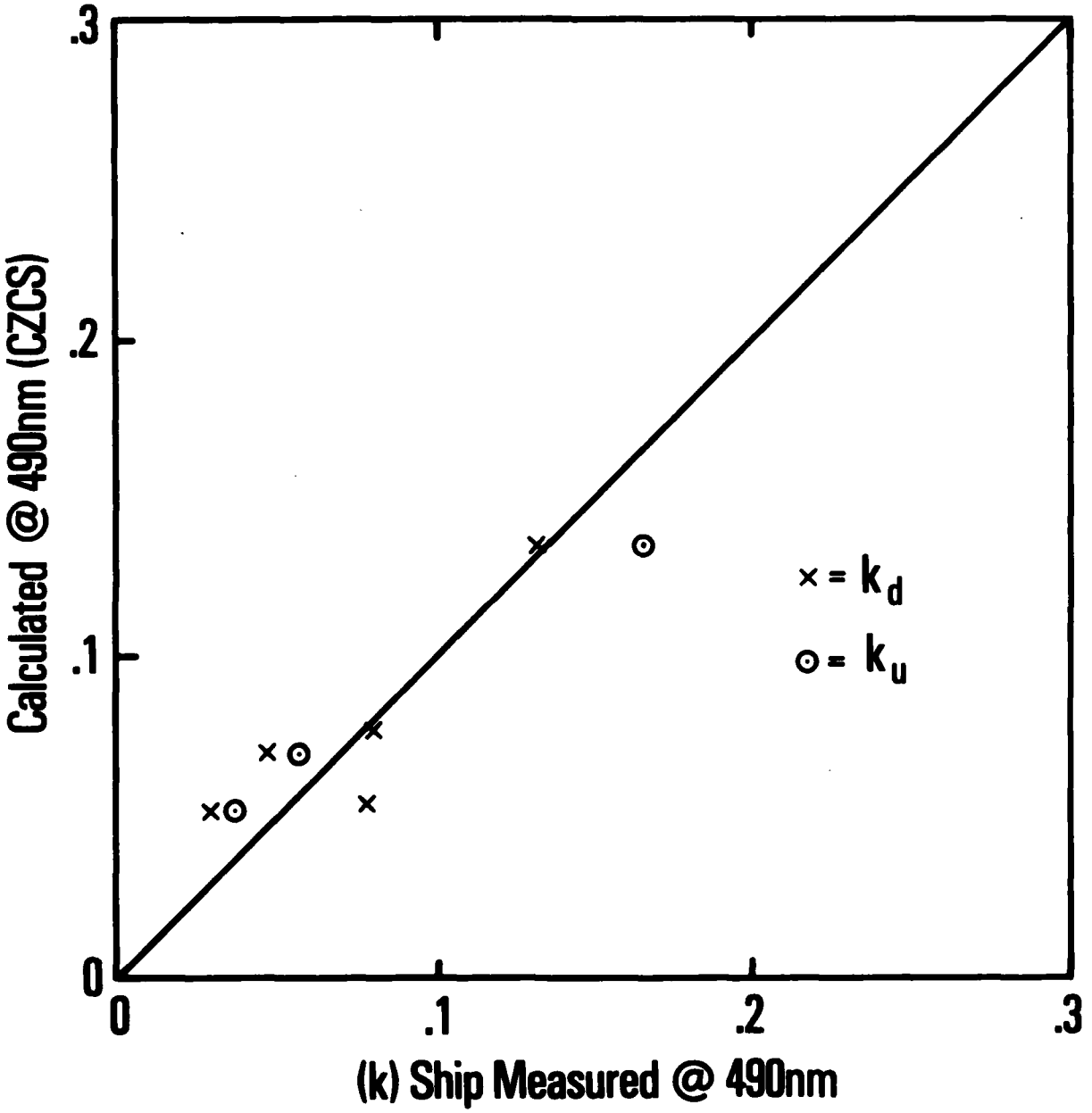

Figure 12: Comparison of ship measurements and Nimbus-7 CZCS calculated diffuse attenuation coefficients.

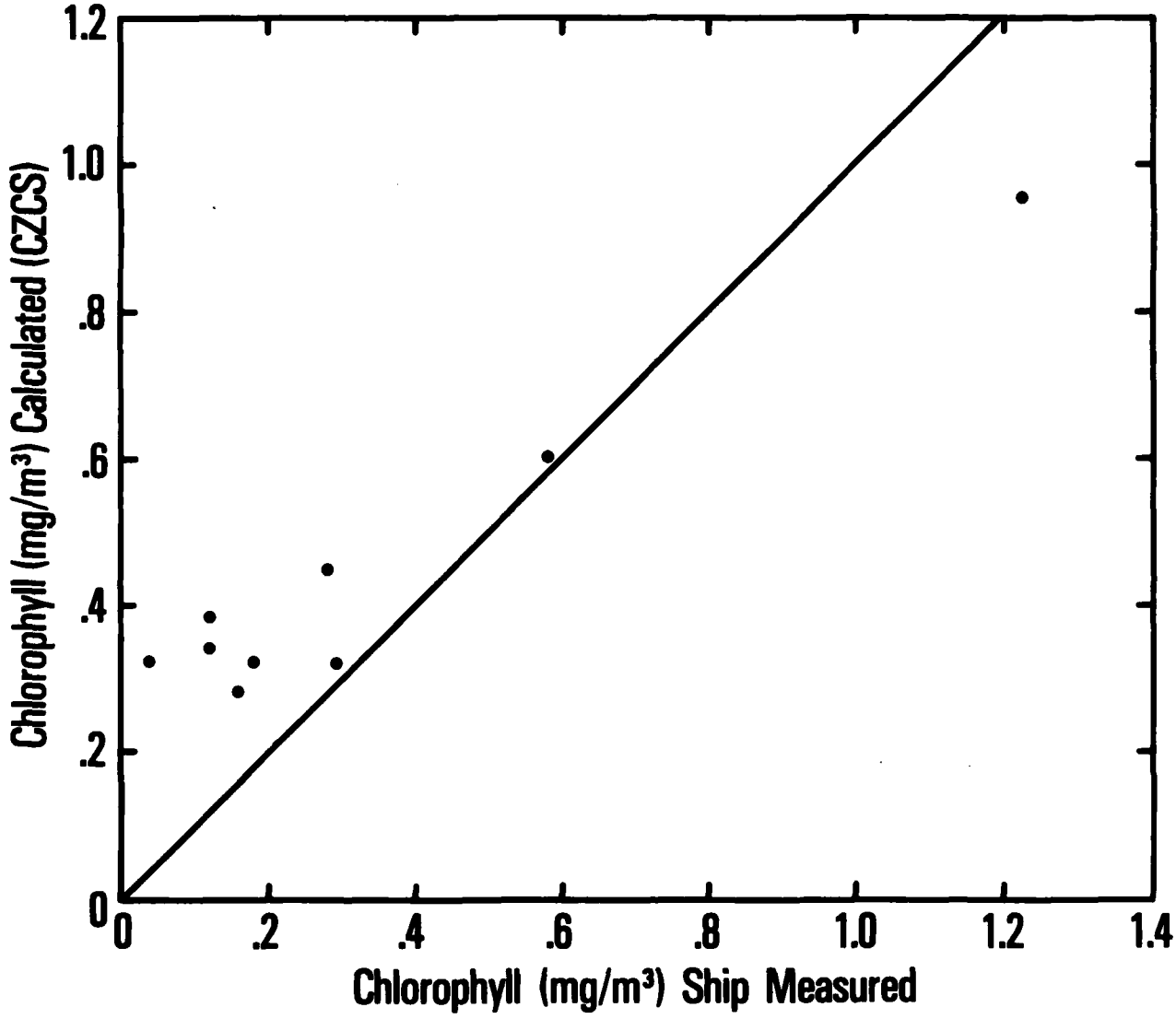

Figure 13: Comparison of ship measurements and Nimbus-7 CZCS calculated phytoplankton concentrations.

good agreement. Similar problems that were discussed for the "k" correlation are also applicable to this figure.

Profiles along the Marbella Line for the 6-day sequence of the satellite-derived sea surface temperature and diffuse attenuation coefficient are shown in Figure 14. The current velocity measurements made by the drift tracks of sonobouys (La Violette, 1983) are also illustrated for 11 and 13 October. A strong correlation between the temperature and optical properties can be observed. Any small lack of correlation between the two satellite data sets can result from several sources. The most obvious of these is the 1-2 km registration error. Not as obvious, but equally a source of any displacement in the two data sets is the fact that the two satellite passes are 2.5 hr apart. The Atlantic inflow water moves rapidly (1.4 m/sec, Kinder 1983) such that the 2.5-hr difference between the CZCS and NOAA-7 passes can result in a noticeable geographic offset in the values computed along the line. Notice that although the positions of the surface thermal fronts have corresponding optical fronts, the sea surface temperatures in the near shore area does not show the high variability shown in the optical properties. Coastal and Atlantic Inflow water masses have similar surface temperatures, yet some distribution can be established by the water color signatures. This is most apparent for the profile for 7 October.

The positions of coastal, Atlantic Inflow, and Alboran Gyre water along the Marbella Line are described by the drift trajectories for 11 and 13 October. The current velocity observed on 11 October indicates a strong north component. These current directions preceeded the leading edge of an eastward advecting turbid, cold water tongue observable in the satellite imagery. On this day a strong eastward component is observed close to the coast coinciding with the maximum temperature and optical front.

The 13 October buoy trajectories indicate that strong eastward velocities that are located approximately 30 km off the coast represent the Atlantic Inflow (this position coincides with the strong temperature and color gradients). It is not possible to establish precise temperature or water color parameters that define the Atlantic Inflow, since the high turbulence imposed by the variable inflow results in strong horizontal and vertical mixing in the upper water column. However, what does appear consistent is that the strong gradients observed in satellite imagery are correlated with the position of the strong eastward velocity measurement.

V. SUMMARY AND CONCLUSIONS

The circulation of the Alboran Sea Gyre has been characterized by a daily sequence of visible (Nimbus-7 CZCS) and thermal IR (NOAA-7 AVHRR) satellite imagery. The atmospherically-corrected and geometrically-registered imagery illustrates the rapid north-south movement of the Atlantic Inflow water as well as associated turbid, cold water tongues that are advected around the Alboran Gyre. The phyto-plankton pigment concentration and the diffuse attenuation coefficient in the upper surface waters have been computed using the ratio of two of the CZCS spectral channels. The mesoscale features characterized by cooler temperatures, higher turbidity, and increased pigment concentration are shown to begin at the Strait of Gibraltar and to move around the Gyre. The Alboran Gyre water is characterized by warm temperatures and very clear water with low pigment concentration.

The quantitative bio-optical properties measured from the Nimbus-7 CZCS are in good agreement with simultaneously collected ship data. The appreciation of utilizing quantitative satellite data for determining the spatial and temporal

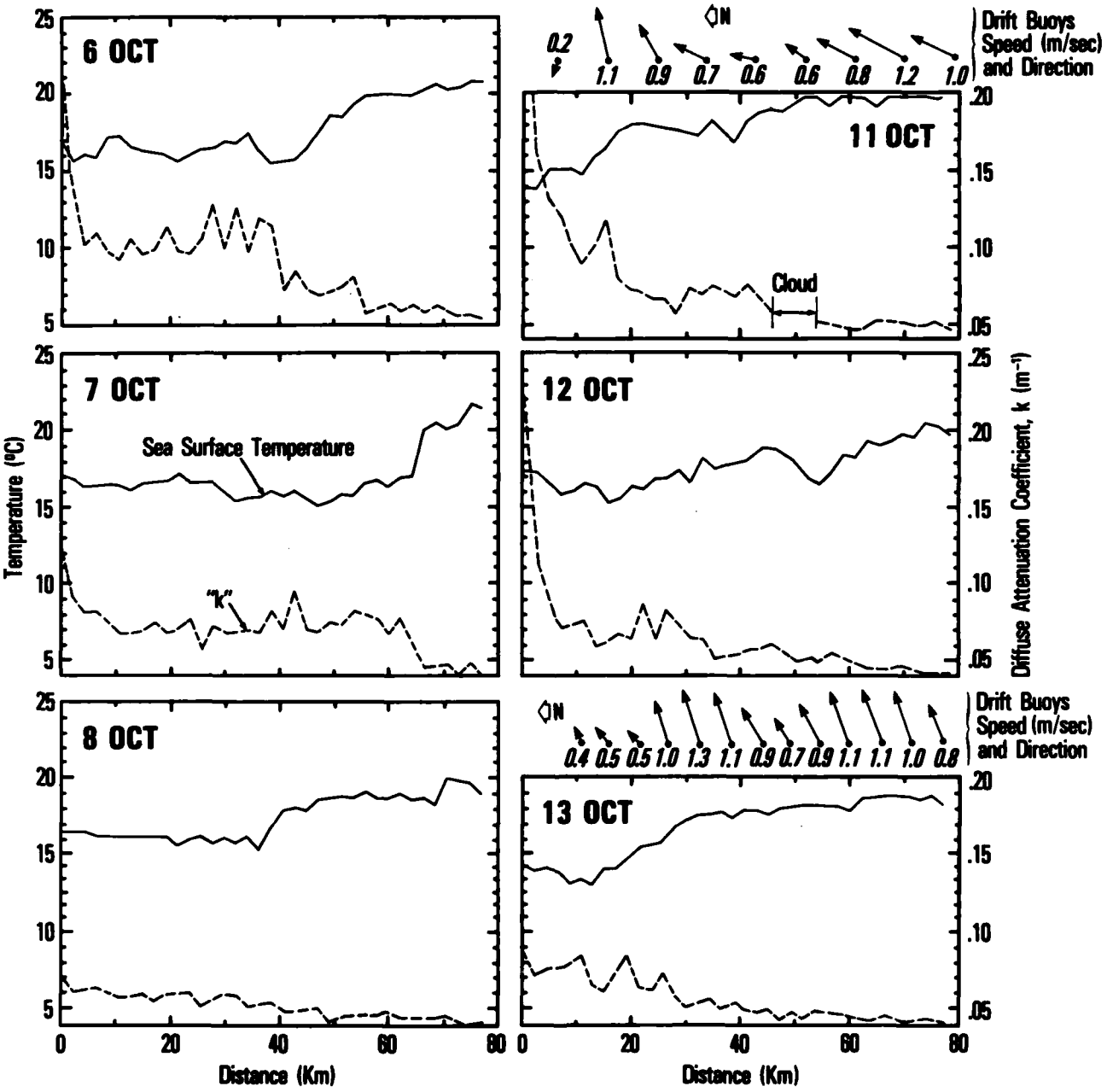

Figure 14: Comparison of CZCS calculated diffuse attenuation coefficients and NOAA-7 AVHRR sea surface temperatures along the Marbella Line with corresponding surface current velocity measurements.

variability of the bio-optical data is demonstrated. The limitations existing in the data because of physical contraints are also shown. The 6-day sequence of visible imagery suggests a high-daily variability of the bio-optical properties occurring along the frontal and coastal water masses. In certain frontal areas a doubling of the diffuse attenuation coefficient apparently occurred within 24 hr.

Ship measurements indicate that the vertical bio-optical distribution is complex within the upper 30 m, and that strong vertical changes occur on a daily basis. Since the satellite signal is limited to the first attenuation length, strong vertical movements of bio-optical properties into and out of this first attenuation length are reflected in the spectral satellite signal, and this vertical movement could be the cause of the changes in values shown by the imagery.

Improved understanding of the variability of bio-optical properties in frontal areas is required. The upwelling spectral radiance should be correlated with the bio-optical properties in order to improve our understanding of the remote sensing of water color.

REFERENCES

Arnone, R. A., Evaluation of CZCS and landsat for coastal optical and water properties, 17th International Symposium on Remote Sensing of Environment, Ann Arbor, MI, 1983a.

Arnone, R. A., Water optics of mississippi sound, Naval Ocean Research and Development Activity (NORDA) Report 63, 1983b.

Arnone, R. A. and R. J. Holyer, Interactive technique for removal of atmospheric contamination in CZCS imagery (Naval Ocean Research and Development Activity Report in preparation), 1984.

Austin, R. W., NIMBUS experimental team report 18, 1982.

Austin, R. W. and T. J. Petzold, The determination of the diffuse attenuation coefficient of sea water using the coastal zone color scanner, Oceanography from Space, ed. J. F. R. Gower, Plenum Publishing Corporation, p. 239, 1980.

Cullen, J. J. and R. W. Eppley, Chlorophyll maximum layers of the southern California bight and possible mechanisms of their formation and maintenance, Oceanol. Acta 4, 1, 23-32, 1981.

Garcia, C. Y. and J. M. Cabanas and D. Cortes, First results of nutrients and chlorophylls during the oceanographic cruise ?Donde Va? in the Alboran Sea, October 1982, ?Donde Va? Meeting Report. Fuengirola. Instituto Espanol de Oceanografia (extended abstracts in English, short abstracts in Spanish and English) ed. by G. Parrilla.

Gordon, H. R., Removal of atmospheric effects from satellite imagery of the oceans, Applied Optics v. 17, p. 1631-1636, 1978.

Gordon, H. R. and D. K. Clark, Atmospheric effects in remote sensing of phytoplankton pigments, Boundary Layer Meteorology, v. 18, p. 299-313, 1980.

Gordon, H. R. and D. K. Clark, Remote sensing optical properties of a stratified ocean: an improved interpretation, Appl. Opt. 19, 3428, 1980.

Gordon, H. R. and D. K. Clark, Clear water radiances for atmospheric correction of coastal zone color scanner imagery, Applied Optics, v. 20, n. 24, p. 4175-4180, 1981.

Gordon, H. R. and W. R. McCluney, Estimation of the depth of sunlight penetration in the sea in remote sensing, Applied Optics, v. 14, n. 2, p. 413-46, 1975.

Gordon, H. R., D. K. Clark, J. W. Brown, O. B. Brown, R. H. Evans and W. W. Broenkow, Phytoplankton pigment concentration in the middle atlantic bight; comparison of ship determination and CZCS estimates, Applied Optics, v. 22, 20, 1983.

Hovis, W. A., D. K. Clark, F. Anderson, R. W. Austin, W. A. Wilson, E. I. Butler, D. Ball, H. R. Gordon, J. L. Mueller, S. F. El-Sayed, B. Sturm, R. C. Wrigley and C. Yentsch, Nimbus-7 coastal zone color scanner: system description and initial imagery, Science, v. 210 (4465) p. 60-63, 1980.

Kinder, T. H., ?Donde va? an oceanographic experiment near the Strait of Gibraltar, Proceedings of IAPSO/ONR/NEFKD Workshop on Straits Inst. Phys. Ocean., Copenhagen, Denmark, 1983.

Lanoix, F., Project Alboran. Etude hydrologigue et dynamique de la Mer d'Alboran, NATO Technical Report 66, p. 36 and 32 figures, 1974.

La Violette, P. E., T. H. Kinder, R. Preller, and H. E. Hurlburt, ?Donde va?: a mesoscale flow dynamics experiment in the Straits of Gibraltar and Alboran Sea, XXVIII Congress and Plenary Assembly of ICSEM, Cannes, France, December 2-11, 1982 (in proceedings), 1982.

La Violette, P. E., The advection of the submesoscale thermal features in the Alboran Sea gyre, Journal Physical Oceanography, v. 13, 2, 1984.

La Violette, P. E. and J. L. Kerling, An analyses of aircraft data collected in the Alboran Sea during ?Donde va? 6 through 18 October 1982, Naval Oceanography Research and Development Activity (NORDA) Technical Note 222, 1983.

Parrilla, G. and T. H. Kinder, The physical oceanography of the Alboran Sea, NATO Advanced Research Workshop, Santa teresa, Italy, September 1983, in proceeding 1984.

Smith, R. C. and W. H. Wilson, Ship and satellite bio-optical research in the California bight. Oceanography from Space, ed J. F. R. Gower, Plenum Publishing Corporation, p. 281, 1981.

Sun, Y. Y., Corrections for inflight calibration of the coastal zone color scanner, International Journal of Remote Sensing, v. 4, p. 829-834, 1983.

UNCLASSIFIED

SECURITY CLASSIFICATION OF THIS PAGE (When Data Entered)

REPORT DOCUMENTATION PAGE		READ INSTRUCTIONS BEFORE COMPLETING FORM
1. REPORT NUMBER NORDA Technical Note 283	2. GOVT ACCESSION NO.	3. RECIPIENT'S CATALOG NUMBER
4. TITLE (and Subtitle) Bio-Optical Variability in the Alboran Sea as Assessed by Nimbus-7 Coastal Zone Color Scanner		5. TYPE OF REPORT & PERIOD COVERED Final 6. PERFORMING ORG. REPORT NUMBER
7. AUTHOR(s) Paul La Violette Robert Arnone		8. CONTRACT OR GRANT NUMBER(s)
9. PERFORMING ORGANIZATION NAME AND ADDRESS Naval Ocean Research & Development Activity Ocean Science Directorate NSTL, Mississippi 39529		10. PROGRAM ELEMENT, PROJECT, TASK AREA & WORK UNIT NUMBERS PE 62759N WF 59553
11. CONTROLLING OFFICE NAME AND ADDRESS Naval Ocean Research & Development Activity Ocean Science Directorate NSTL, Mississippi 39529		12. REPORT DATE August 1984 13. NUMBER OF PAGES 29
14. MONITORING AGENCY NAME & ADDRESS(if different from Controlling Office)		15. SECURITY CLASS. (of this report) Unclassified 15a. DECLASSIFICATION/DOWNGRADING SCHEDULE

16. DISTRIBUTION STATEMENT (of this Report)

Approved for Public Release
Distribution Unlimited

17. DISTRIBUTION STATEMENT (of the abstract entered in Block 20, if different from Report)

18. SUPPLEMENTARY NOTES

19. KEY WORDS (Continue on reverse side if necessary and identify by block number)

Donde Va?
CZCS data
Nimbus-7
Alboran Sea

20. ABSTRACT (Continue on reverse side if necessary and identify by block number)

An international oceanographic experiment, Donde Va?, was conducted in 1982 in the Alboran Sea in which a specialized portion was dedicated to examining the spatial and temporal variability of bio-optical properties around the Alboran Sea Gyre. The circulation of the Alboran Sea, as characterized by Atlantic Inflow (through the Strait of Gibraltar), the Alboran Gyre, and coastal water masses, was analyzed through use of Nimbus-7 Coastal Zone Color Scanner (CZCS) imagery, NOAA-7 Advanced Very High Resolution Radiometer (AVHRR

DD FORM 1 JAN 73 1473 EDITION OF 1 NOV 65 IS OBSOLETE
S/N 0102-LF-014-6601

UNCLASSIFIED
SECURITY CLASSIFICATION OF THIS PAGE (When Data Entered)

imagery, and aircraft and ship data. Diffuse attenuation coefficients calculated from CZCS data are in agreement with the ship data. A strong correlation between the surface temperature and ocean color fronts was observed in the two satellite imagery sets.

A 6-day sequence of CZCS imagery shows that significant changes in the diffuse attenuation coefficient and phytoplankton pigment concentration occurred in the frontal regions. These changes are attributed to the bio-optical horizontal and vertical variations that occurred within the first attenuation length.

END

FILMED

1-85

DTIC